

Study of integrated and transverse momentum differential production rates for particles emitted in high energy collisions at the LHC

G. Coulon and A. Dedieu

Université de Strasbourg, IPHC, 23 rue du Loess 67037 Strasbourg, France

(Dated: February 15, 2023)

In this paper are compared various fitted functions applied to production rates of (anti)protons and ϕ mesons, obtained from the most central proton and lead collisions at the LHC. Boltzmann and power law fits are first tried, and more specific functions are then used, namely a Lévy-Tsallis one for proton collisions, and a hydrodynamic blast-wave model for lead collisions. Fits show very good agreement with data and their parameters are consistent with those of the literature. 1 and 2- σ contours are then plotted for the temperature with respect to the mean transverse velocity distribution of the blast-wave model, again consistent with the literature.

INTRODUCTION

One of the goals of collider experiments such as ALICE¹ in the LHC²(where the data to be analyzed here is extracted), is to obtain the momentum distribution of emitted particles during a collision. This is particularly useful for characterising collisions and know precisely what background to expect when performing further measurements. Due to the cylindrical geometry of most detectors, including ALICE, the momentum of emitted particles can be written as : $\vec{p} = p_T \vec{t} + p_L \vec{l}$, where p_T and p_L are the transverse and longitudinal components of the momentum respectively, corresponding to the transverse \vec{t} and longitudinal \vec{l} directions with respect to the proton (pp) or lead (Pb-Pb) beams. The focus here is on the transverse part of the momentum, for mainly two reasons : it is easier to measure, and because of the composite nature of collided objects, one does not know precisely the energy involved in the longitudinal plan for each collision, yet can make the hypothesis of no momentum in the transverse plan except for that coming from collisions. The quantity of interest in this paper is then the number of particles created, for a given rapidity y and a given transverse momentum p_T , noted $dN/dydp_T$. However, the magnetic field needed for determining the momentum leads to an inefficiency at low p_T , because particles trajectories are curved by the magnetic field, and for the lowest p_T , particles do not get enough speed to reach detectors and keep spinning close to the primary vertex of the collision. As a consequence, most detectors are blind to this low p_T region (typically here, under 0.3 or 0.4 GeV) and the best fitted functions are required to modelize the data and extrapolate the distribution for low p_T . We report in this paper a comparison of several fits to these production rates, supported by physics arguments, for (anti)protons, and ϕ mesons, with similar masses, produced both in pp and Pb-Pb collisions

at $\sqrt{s_{NN}} = 5.02$ TeV at the LHC, with the associated extrapolated yields for low p_T . 1 and 2- σ contours are then plotted for the so-called blast-wave fit, providing informations on the temperature of quark-gluon plasma created in accelerators.

DATA MODELING

The data used in this paper is extracted from [11][12] and concerns the production of (anti)protons and ϕ mesons in both pp and Pb-Pb collisions. The uncertainties provided (statistical and systematic) are propagated in an uncorrelated manner. Several fits were performed and the aim of this section is to describe the motivation for each of them. As it can be seen in Figures 1 and 3 the typical shape for the production rate of particles as a function of p_T is a peak at low p_T and a stiff decrease towards higher p_T . This behaviour can be explained by the fact that low p_T particles have a higher probability to be created during a collision, and that high p_T particles tend to quickly decay into lower p_T ones, giving this characteristic shape, with particles hugely majoritarian in low p_T . The peak is very well modelised by a Boltzmann distribution (1)[5], and the decreasing part by a power law (3)[7], as shown for Pb-Pb collisions in Figure 1. Each time m appears, it corresponds to the mass of produced particles (0.938 GeV for protons, 1.020 GeV for ϕ mesons), and m_T is the transverse mass, defined in equation (2). Greek letters are normalisation constants, and for Boltzmann distribution, T is the temperature at which the resonance occurs.

$$\frac{d^2 N}{dy dp_T} = \alpha \cdot p_T \cdot m_T \cdot \exp(-m_T/T) \quad (1)$$

$$m_T = \sqrt{m^2 + p_T^2} \quad (2)$$

$$\frac{d^2 N}{dy dp_T} = \alpha + \beta \cdot p_T^n \quad (3)$$

¹ A Large Ion Collider Experiment

² Large Hadron Collider

The high number of partons involved in Pb-Pb collisions and the high number of particles thus created also allows one to modelise the production rate with hydrodynamic models, such as the blast-wave one (4)[1][8]. Like the Boltzmann distribution, this fit is suited for the low p_T peak, and it represents the colliding system as a blasting fireball of radius R . T is the temperature at the kinetic freeze-out and β_S is the transverse expansion velocity of the fireball. β_T is then the transverse velocity distribution in the region $0 < r < R$. Finally, K_0 and I_1 are the modified Bessel functions.

$$\frac{d^2N}{dydp_T} = \alpha \int_0^R p_T m_T I_0 \left(\frac{p_T \sinh(\rho)}{T} \right) K_1 \left(\frac{m_T \cosh(\rho)}{T} \right) r dr \quad (4)$$

$$\rho = \tanh^{-1} \beta_T = \tanh^{-1} \left[\left(\frac{r}{R} \right)^n \beta_S \right] \quad (5)$$

For pp collisions, another approach can be taken, by combining an exponential shape, useful for low p_T , characterized by a temperature parameter T , and a power law one (n being the power parameter), describing the higher p_T region. This combination is called the Lévy-Tsallis function [6], and this approach is particularly interesting because the fit is then effective on the whole p_T range.

$$\frac{d^2N}{dydp_T} = \frac{(n-1)(n-2)}{nT[nT + m(n-2)]} \frac{dN}{dy} p_T \left(1 + \frac{m_T - m}{nT} \right)^{-n} \quad (6)$$

FIT RESULTS AND YIELD EXTRAPOLATION

Before going to the results, it is important to have in mind the discussion of reference [4] : when working with a binned distribution, the appropriate place to plot data points is neither the barycentre nor the centre value of the bin, but the place where the fit function is equal to its mean value over the bin. This fact is taken into account in ROOT via the parameter “I” in the fit methods. For the Boltzmann, power, and Lévy-Tsallis fits, the initialisation of parameters is not critical and a convergence point is typically reached in a few seconds. The important point is the fit range, because as we said the various functions do not apply to the same p_T range. We chose to perform Boltzmann fits from the low edge of the first bin (0.3 or 0.4 GeV) until 2 GeV, and power law fits from 8 to 18 GeV ($p + \bar{p}$) and from 5 to 18 GeV (ϕ). We applied Lévy-Tsallis on the whole p_T range. Results for (anti)protons are shown in Figures 1 and 3, and the obtained parameters and yield extrapolated fraction are shown in Table I. The χ^2/NDF (shown in corresponding figures) are satisfactory, showing these functions are able to model well the data. Lévy-Tsallis parameters are of the same order of magnitude as those in the literature but sometimes differ by up to a factor of 2 [6].

p_T distribution of $p+\bar{p}$ measured in Pb-Pb collisions at $\sqrt{s_{NN}}=5.02$ TeV with 0-5 % centrality

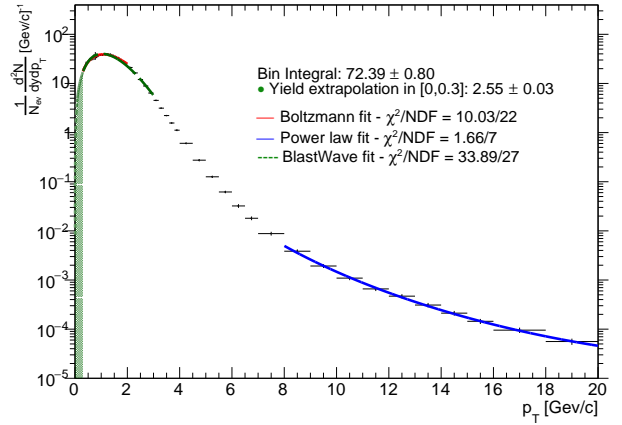


Figure 1. p_T distribution of $p+\bar{p}$ measured in Pb-Pb collisions at $\sqrt{s_{NN}} = 5.02$ TeV with 0-5% centrality. A Boltzmann distribution and a power law are fitted to the data, along with a blast-wave model. The green part corresponds to the extrapolated yield.

p_T distribution of $p+\bar{p}$ measured in Pb-Pb collisions at $\sqrt{s_{NN}}=5.02$ TeV with 0-5 % centrality

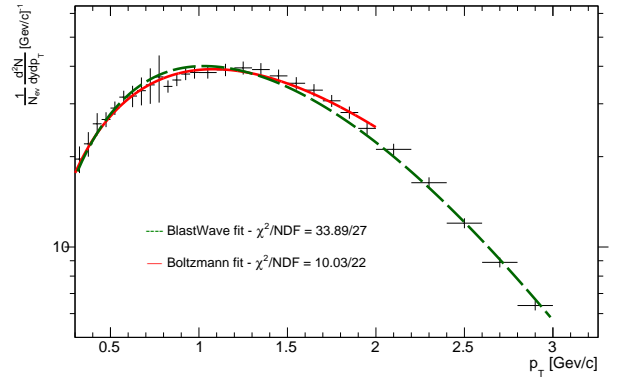


Figure 2. p_T distribution of $p+\bar{p}$ measured in Pb-Pb collisions at $\sqrt{s_{NN}} = 5.02$ TeV with 0-5% centrality, zoomed in the low p_T region

On the other hand, blast-wave fits are much more complex to compute because of the integral calculation and the greater number of parameters. This is why we chose to take the parameters obtained in the literature [1] as a starting point, for the computing not to take more than a few minutes. Results are shown in Figure 1 and Table I. The parameters obtained are thus very close to the ones of the literature, except for the normalisation one which is unexplainedly high.

CONTOURS

Finally, we also drew 1 and 2- σ contours for the T and $\langle\beta_T\rangle$ parameters of the blast-wave function applied to the

p_T distribution of $p + \bar{p}$ measured in pp collisions at $\sqrt{s_{NN}} = 5.02$ TeV with 0-5% centrality

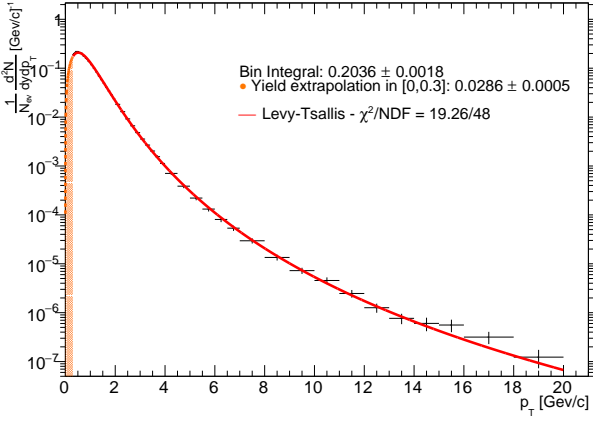


Figure 3. p_T distribution of $p + \bar{p}$ measured in pp collisions at $\sqrt{s_{NN}} = 5.02$ TeV with 0-5% centrality. A Lévy-Tsallis distribution is fitted to the data. The orange part corresponds to the extrapolated yield.

| Distribution law | Parameters | Extrapolated over total yield (%) |
|------------------|---|-----------------------------------|
| Boltzmann | $\alpha = 396 \pm 19$ $T = 0.520 \pm 0.009$ | |
| Power | $\alpha = 1.31 \cdot 10^{-5} \pm 1.30 \cdot 10^{-5}$ $\beta = 434 \pm 284$ $n = -5.47 \pm 0.28$ | |
| Blast-wave | $\alpha = 8.32 \cdot 10^5$ (fixed) $T = 0.08998 \pm 0.00008$ $n = 0.735$ (fixed) $\langle \beta_T \rangle = 0.664 \pm 0.001$ | 3.52 ± 0.06 |
| Lévy-Tsallis | $n = 7.81 \pm 0.09$ $T = 0.230 \pm 0.002$ $\frac{dN}{dy} = 0.231 \pm 0.002$ | 14.05 \pm 0.26 |
| Boltzmann | $\alpha = 930 \pm 15$ $T = 0.504 \pm 0.024$ | 6.92 ± 0.47 |
| Power | $\alpha = 3.41 \cdot 10^{-5} \pm 1.22 \cdot 10^{-5}$ $\beta = 176 \pm 69$ $n = -5.28 \pm 0.19$ | |
| Lévy-Tsallis | $n = 7.62 \pm 0.18$ $T = 0.310 \pm 0.007$ $\frac{dN}{dy} = 0.0289 \pm 0.0007$ | 15.75 \pm 0.87 |

Table I. Fitted functions parameters and associated yield extrapolated fraction, for the most central events. Boltzmann, power, and blast-wave fits concern Pb-Pb collisions and Lévy-Tsallis concerns pp ones. Upper part : $p + \bar{p}$. Lower part : ϕ

production of (anti)protons. A quick integral calculation gives (7). The contours are shown in Figures 4 and 5. The shape is the same as the one obtained in [1], but the contours are smaller because we only consider here (anti)protons.

$$\langle \beta_T \rangle = \frac{2}{n+2} \beta_S \quad (7)$$

The curve tends to become flat for the lowest $\langle \beta_T \rangle$,

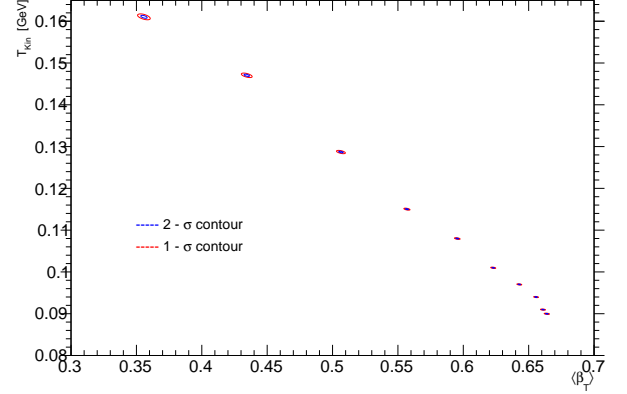


Figure 4. Shape of the 1 and 2- σ contours for T with respect to $\langle \beta_T \rangle$ in the case of a blast-wave fit for $p + \bar{p}$ production in Pb-Pb collisions. High T values correspond to low centrality

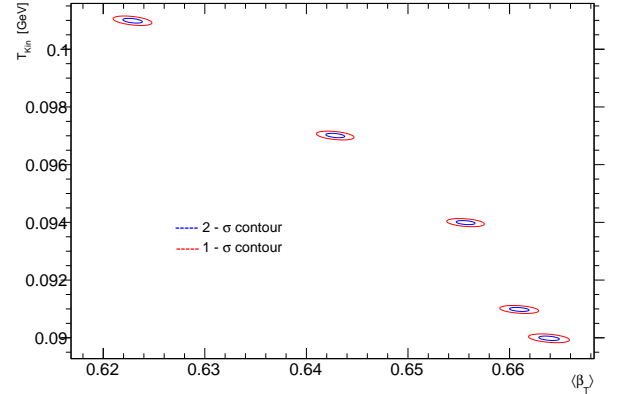


Figure 5. 1 and 2- σ contours for T with respect to $\langle \beta_T \rangle$ in the case of a blast-wave fit for $p + \bar{p}$ production in Pb-Pb collisions, zoomed in the most central events region

corresponding to temperatures of about 150 to 160 MeV, which is consistent with the usual temperature of quark-gluon plasma produced in particle accelerators. At this temperature, there is no more hadron and this is why we can not go further on the contours curve.

CONCLUSION

Several fits were performed on (anti)protons and ϕ mesons production rates, in Pb-Pb and pp collisions at the LHC. χ^2/NDF values show very good agreement with data, in particular for Lévy-Tsallis applied to pp collisions, and the obtained parameters and extrapolated yields are consistent with the ones obtained in the previous literature. Finally, 1 and 2- σ contours were drawn for the blast-wave fit, again consistent with the reference articles.

-
- [1] S. Acharya et al. (ALICE Collaboration), “Production of charged pions, kaons, and (anti-)protons in Pb-Pb and inelastic pp collisions at $\sqrt{s_{NN}} = 5.02$ TeV”, Phys. Rev. C 101 (2020) 4, 04490, <http://arxiv.org/abs/arXiv:1910.07678>.
 - [2] S. Acharya et al. (ALICE Collaboration), “Evidence of rescattering effect in Pb-Pb collisions at the LHC through production of $K^*(892)^0$ and $\phi(1020)$ mesons”, Phys. Lett. B 802 (2020), 135225, <http://arxiv.org/abs/arXiv:1910.14419>.
 - [3] S. Wheaton and J. Cleymans, “THERMUS: A Thermal model package for ROOT”, Comput. Phys. Commun. 180 (2009), 84–106, <https://arxiv.org/abs/hep-ph/0407174>.
 - [4] G.D. Lafferty and T.R. Wyatt, “Where to stick your data points: the treatment of measurements within wide bins”, Nucl. Instrum. Meth. A355 (1995) 541, CERN-PPE-94-072, May 1994. 17pp.
 - [5] J. Adams et al. (STAR Collaboration), “ $K(892)^*$ Resonance Production in Au+Au and p+p Collisions at $\sqrt{s_{NN}} = 200$ GeV at STAR”, Phys. Rev. C71 (2005) 064902, <http://arxiv.org/abs/nuc1-ex/0412019>.
 - [6] K. Aamodt et al. (ALICE Collaboration), “Strange particle production in proton-proton collisions at $\sqrt{s_{NN}} = 0.9$ TeV with ALICE at the LHC”, Eur. Phys. J. C71 (2011) 1594, <http://arxiv.org/abs/arXiv:1012.3257>.
 - [7] S. Acharya et al. (ALICE Collaboration), “Studies of J/ψ production at forward rapidity in Pb-Pb collisions at $\sqrt{s_{NN}} = 5.02$ TeV”, JHEP 02 (2020), 041, <http://arxiv.org/abs/arXiv:1909.03158>.
 - [8] E. Schnedermann, J. Sollfrank and U. Heinz, “Thermal phenomenology of hadrons from 200-A/GeV S+S collisions.”, Phys. Rev. C48 (1993) 2462, <http://arxiv.org/abs/nuc1-th/9307020>.
 - [9] F. R  ti  re and M.A. Lisa, “Observable implications of geometrical and dynamical aspects of freeze out in heavy ion collisions.”, Phys. Rev. C70 (2004) 044907, <http://arxiv.org/abs/nuc1-th/0312024>.
 - [10] S. Borsanyi et al., “Is there still any T_c mystery in lattice QCD? Results with physical masses in the continuum limit III”, JHEP 09 (2010) 073, <http://arxiv.org/abs/arXiv:1005.3508>.
 - [11] Data : $p + \bar{p}$ production <https://www.hepdata.net/record/sandbox/1569102768>
 - [12] Data : ϕ production <https://www.hepdata.net/record/ins1762368>
 - [13] Github link to the projet : <https://github.com/glcln/TIPP2023>